ORIGINAL RESEARCH

LPS-induced Acute Lung Injury Involves NF-κB–mediated Downregulation of SOX18

Christine M. Gross[1], Manuela Kellner[2], Ting Wang[2], Qing Lu[2], Xutong Sun[2], Evgeny A. Zemskov[2], Satish Noonepalle[2], Archana Kangath[2], Sanjiv Kumar[1], Manuel Gonzalez-Garay[2], Ankit A. Desai[2], Saurabh Aggarwal[3], Boris Gorshkov[1], Christina Klinger[2], Alexander D. Verin[1], John D. Catravas[4], Jeffrey R. Jacobson[5], Jason X.-J. Yuan[2], Ruslan Rafikov[2], Joe G. N. Garcia[2], and Stephen M. Black[2]

[1]Vascular Biology Center, Augusta University, Augusta, Georgia; [2]Department of Medicine, The University of Arizona Health Sciences, Tucson, Arizona; [3]Department of Anesthesiology and Perioperative Medicine, The University of Alabama at Birmingham School of Medicine, Birmingham, Alabama; [4]Frank Reidy Research Center for Bioelectrics, Old Dominion University, Norfolk, Virginia; and [5]Department of Medicine, University of Illinois College of Medicine, Chicago, Illinois

Abstract

One of the early events in the progression of LPS-mediated acute lung injury in mice is the disruption of the pulmonary endothelial barrier resulting in lung edema. However, the molecular mechanisms by which the endothelial barrier becomes compromised remain unresolved. The SRY (sex-determining region on the Y chromosome)–related high-mobility group box (Sox) group F family member, SOX18, is a barrier-protective protein through its ability to increase the expression of the tight junction protein CLDN5. Thus, the purpose of this study was to determine if downregulation of the *SOX18-CLDN5* axis plays a role in the pulmonary endothelial barrier disruption associated with LPS exposure. Our data indicate that both SOX18 and CLDN5 expression is decreased in two models of *in vivo* LPS exposure (intraperitoneal, intratracheal). A similar downregulation was observed in cultured human lung microvascular endothelial cells (HLMVECs) exposed to LPS. SOX18 overexpression in HLMVECs or in the mouse lung attenuated the LPS-mediated vascular barrier disruption. Conversely, reduced CLDN5 expression (siRNA) reduced the HLMVEC barrier-protective effects of SOX18 overexpression. The mechanism by which LPS decreases SOX18 expression was identified as transcriptional repression through binding of NF-κB (p65) to a SOX18 promoter sequence located between −1,082 and −1,073 bp with peroxynitrite contributing to LPS-mediated NF-κB activation. We conclude that NF-κB–dependent decreases in the *SOX18-CLDN5* axis are essentially involved in the disruption of human endothelial cell barrier integrity associated with LPS-mediated acute lung injury.

Clinical Relevance

Our data demonstrate a previously unknown role for the Sox18–claudin-5 axis in the development of acute lung injury (ALI). Increasing the expression of Sox18 in either cultured endothelial cells or the mouse endothelium protects against the ALI associated with LPS exposure. Sox18 may be a novel target for treating ALI.

(Received in original form November 28, 2016; accepted in final form November 8, 2017)

Supported in part by grants HL60190 (S.M.B.), HL67841 (S.M.B.), HL101902 (S.M.B.), P01HL134610 (S.M.B.), HL126609 (J.G.N.G.), HL115014 (J.X.-J.Y.), HL096887 (J.R.J.), and HL132918 (R.R.), all from the National Institutes of Health (NIH), and by a Scientist Development Grant (14SDG20480354 [R.R.]) from the American Heart Association National Office.

Author Contributions: Conception and design: C.M.G., M.K., T.W., E.A.Z., S.N., A.K., S.A., A.D.V., J.G.N.G., and S.M.B.; analysis and interpretation: C.M.G., M.K., T.W., Q.L., X.S., E.A.Z., S.N., A.K., S.K., M.G.-G., A.A.D., S.A., B.G., C.K., A.D.V., J.D.C., J.R.J., J.X.-J.Y., R.R., J.G.N.G., and S.M.B.; and drafting of the manuscript for important intellectual content: C.M.G., M.K., T.W., Q.L., X.S., E.A.Z., S.N., A.K., A.A.D., A.D.V., J.D.C., J.R.J., J.X.-J.Y., R.R., J.G.N.G., and S.M.B.

Correspondence and requests for reprints should be addressed to Stephen M. Black, Ph.D., Division of Translational and Regenerative Medicine, The University of Arizona Health Sciences, Steele Children's Research Center, Office 7341A, 1501N Campbell Avenue P.O. Box 245002, Tucson, AZ 85724. E-mail: steveblack@e-mail.arizona.edu.

This article has a data supplement, which is accessible from this issue's table of contents at www.atsjournals.org.

Am J Respir Cell Mol Biol Vol 58, Iss 5, pp 614–624, May 2018

Originally Published in Press as DOI: 10.1165/rcmb.2016-0390OC on November 8, 2017
Internet address: www.atsjournals.org

Acute lung injury (ALI) and acute respiratory distress syndrome (ARDS) are characterized by the rapid onset of respiratory insufficiency, resulting in arterial hypoxemia that is refractory to oxygen therapy (1). ALI is considered to be a less severe form of ARDS with moderate hypoxemia and a $Pa_{O_2}/F_{I_{O_2}}$ ratio of less than 300 mm Hg (1). The incidence of ALI has recently been estimated at 86.2 per 100,000 persons per year and its mortality rate at 38.5% (2). The etiologies of ALI/ARDS are divided into two categories: those that cause direct lung injury and those that cause indirect lung injury by activating a systemic inflammatory response (3). Of the various risk factors, sepsis is associated with the highest risk of progression to ARDS (4). Replicating or dying bacteria release antigens into the systemic circulation, including LPS (5), from gram-negative bacteria, triggering a systemic immune response. These microbial products interact with lung endothelial cells lining blood vessels. Vascular endothelial cells exposed to bacterial toxins or inflammatory mediators secrete inflammatory and chemotactic substances, express adhesion molecules, and exhibit a loss of anticoagulant and barrier functions (6). The loss of pulmonary endothelial barrier function is considered to be a major characteristic of ALI/ARDS pathogenesis. The ensuing plasma extravasation leads to pulmonary edema, the hallmark of ALI/ARDS.

LPS disrupts the alveolar–capillary barrier, resulting in pulmonary vascular leak. However, little is known about the transcriptional events in endothelial cells that lead to the destabilization of the paracellular barrier under these conditions. We have recently shown that the transcription factor SOX18 protects the endothelial barrier against the disruptive effects of laminar shear stress by stimulating the expression of the tight junction protein claudin 5 (CLDN5) (7). *SOX18* belongs to the SRY (sex-determining region on the Y chromosome)–related HMG (high-mobility group) box group F family of transcription factors and plays a key role in blood vessel development. Interestingly, mutations in *SOX18* cause cyanosis and superficial hemorrhage, as well as severe edema (8, 9). Thus, we hypothesized that under conditions of ALI, SOX18 expression would be decreased and that the subsequent decrease in CLDN5 would potentially be involved in the increased pulmonary vascular leak in response to LPS.

Our data demonstrate that the *SOX18-CLDN5* axis is decreased in two models of LPS-mediated ALI, with overexpression of SOX18 attenuating the severity of the lung injury induced by LPS challenge. Furthermore, we found that the mechanism by which LPS decreased SOX18 expression occurs via transcriptional repression and is mediated, at least in part, by the transcription factor NF-κB. Thus, our work identifies SOX18 as a new target in the complex regulation of lung vascular barrier function in response to gram-negative bacteria–dependent ALI.

Methods

Animal Studies

All animal housing protocols were approved by the institutional animal care and use committee in facilities accredited by American Association for the Accreditation of Laboratory Animal Care at Augusta University.

LPS-induced Lung Injury Models

Adult male C57BL/6NHsd mice (aged 7–8 wk; Harlan) were used in all experiments as described in the data supplement.

In vivo Overexpression of SOX18

The plasmids, pCMV6-SOX18 (40 μg) or DST-luciferase (40 μg), were incubated with glucose and jetPEI reagent (Polyplus-transfection Inc.) as per the manufacturer's instructions for 15–30 minutes. Then, the DNA–jetPEI complexes were injected into mice via the tail vein as previously described (10).

Cell Culture

Primary cultures of human lung microvascular endothelial cells (HLMVECs) were isolated as described previously (11). Cells were cultured in M199 medium supplemented with 20% FBS, 100 U/ml heparin, 150 μg/ml endothelial cell growth factor, 1 μg/ml hydrocortisone, 292 mg/L L-glutamine, and 110 mg/L sodium pyruvate and maintained at 37°C in a humidifier with 5% CO_2 and 95% air. Cells were subcultured in a 1:3 ratio using standard techniques.

Transient Transfection of HLMVECs

HLMVECs were transfected with pCMV6-SOX18 plasmid or an NF-κB luciferase reporter assay plasmid using Effectene Transfection Reagent (Qiagen) or a Nucleofector 2b electroporator and the HLMVEC Nucleofector Kit (Lonza) according to the manufacturer's instructions.

siRNA-mediated Knockdown

HLMVECs were transfected with 20 nM of SOX18 or CLDN5 siRNA (Santa Cruz Biotechnology) with the use of HiPerFect Transfection Reagent (Qiagen) according to the manufacturer's instructions. A scrambled siRNA was used as a negative control. Validation of the gene-silencing effect was confirmed by immunoblot analysis. Additional methods used are described in the data supplement.

Statistical Analysis

Statistical analysis was performed using Prism version 4.01 software (GraphPad Software). The mean ± SEM was calculated in all experiments, and statistical significance was determined by an unpaired *t* test (for two groups), one-way analysis of variance (for three or more groups) with Newman-Keuls *post hoc* testing, or two-way analysis of variance with Bonferroni *post hoc* testing. A value of $P < 0.05$ was considered significant.

Results

Expression of SOX18 and CLDN5 Are Reduced in a Mouse Model of ALI and in HLMVECs

A previous study showed that *SOX18* expression is reduced in human umbilical vein endothelial cells by the proinflammatory mediators TNF-α, IL-1, and LPS (12). Therefore, we hypothesized that LPS dysregulates *SOX18* expression and that this mechanism is involved, at least in part, in the disruption of the endothelial barrier and edema formation in ALI. We first confirmed the downregulation of *Sox18* at the mRNA (Figure 1A) and protein (Figure 1B) levels in the lungs of mice treated with LPS intraperitoneally for the indicated amount of time. In HLMVECs exposed to LPS (1 endotoxin unit [EU]/ml; 4 h), *SOX18* mRNA (Figure 1C) and protein (Figure 1D) levels were similarly reduced. We have

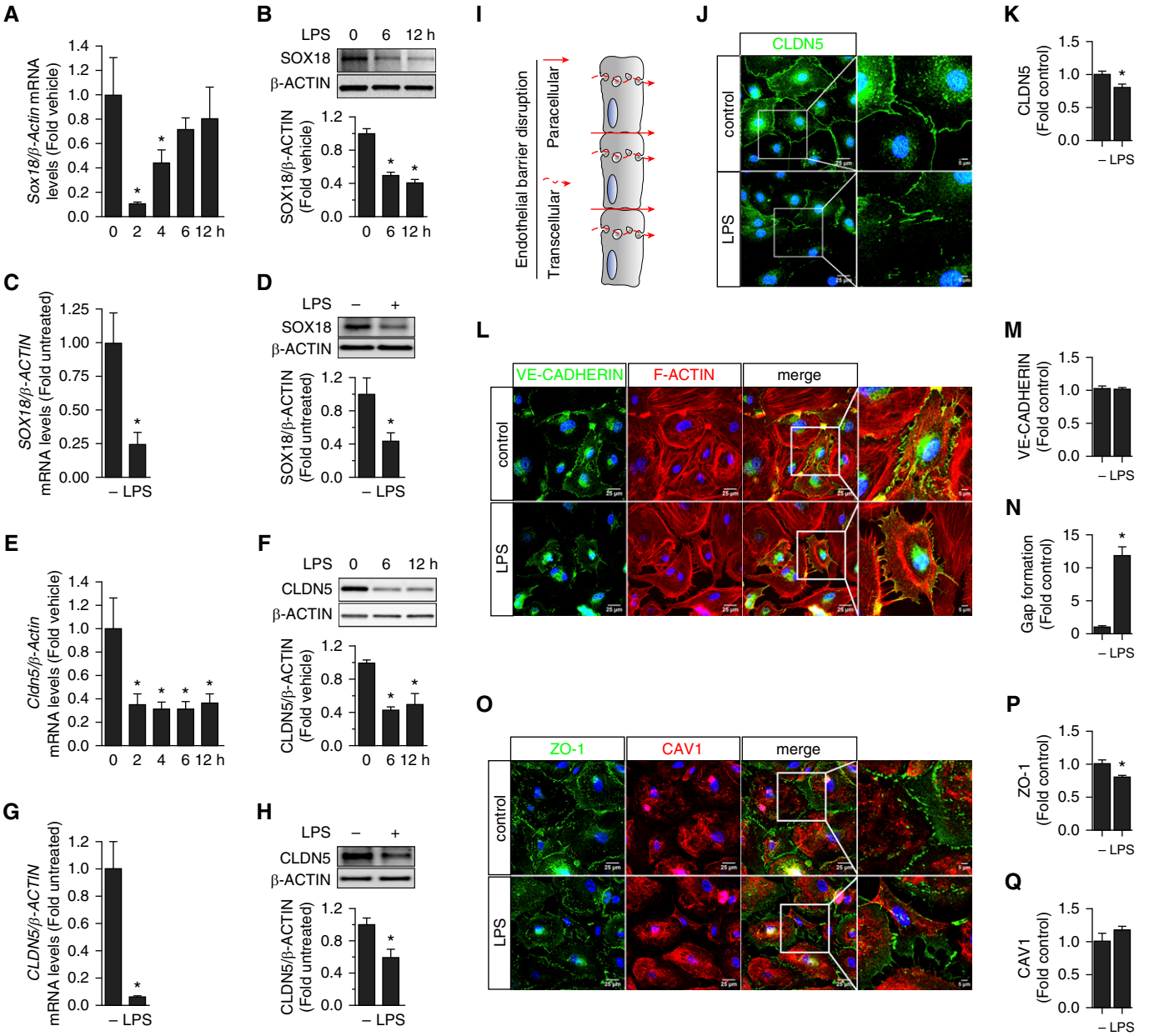

Figure 1. LPS exposure reduces *SOX18* and *CLDN5* expression in the mouse lung and in human lung microvascular endothelial cells (HLMVECs). *In vivo* studies were conducted in which mice were treated with LPS (6.75×10^4 endotoxin units [EU]/g) intraperitoneally for up to 12 hours, and *in vitro* studies were performed using HLMVECs exposed to LPS (4 h; 1 EU/ml). Total RNA was isolated from LPS-treated mouse lungs and HLMVECs. (*A* and *E*) mRNA levels for *Sox18* and *Cldn5* were significantly decreased in mice treated with LPS compared with vehicle-treated mice, as determined by SYBR Green real-time RT-PCR analysis. Protein extracts prepared from lung tissue homogenates were subjected to immunoblot analysis and probed with anti-SOX18 or anti-CLDN5 antibodies. (*B* and *F*) Densitometric analysis indicated that SOX18 and CLDN5 protein levels were reduced in mice exposed to LPS. Furthermore, HLMVECs exposed to LPS for 4 hours had significantly lower (*C* and *G*) *SOX18* and *CLDN5* mRNA expression, as determined by SYBR Green real-time RT-PCR analysis, as well as (*D* and *H*) protein levels, as indicated by immunoblot analysis. (*I*) HLMVECs were exposed or not to LPS for 3 hours (1 EU/ml), and changes in paracellular and transcellular pathways were evaluated using immunofluorescence to detect (*J* and *K*) CLDN5, (*L* and *M*) vascular endothelial cadherin (VE-cadherin), (*O* and *P*) ZO-1, or (*O* and *Q*) CAV1. (*L* and *N*) Cells were also simultaneously stained with phalloidin and demonstrated an increase in gap formation. LPS decreased CLDN5 levels significantly. (*L* and *M*) Total VE-cadherin levels were unchanged, but the cell border localization was attenuated. LPS significantly decreased ZO-1 levels (*O* and *P*), but CAV1 levels were unchanged (*O* and *Q*). Values are mean ± SEM; $n = 4$–6. Scale bars (panels *L* and *O*): 25 μm except in the right-hand panels, which are 5 μm. *$P < 0.05$ versus no LPS. CAV1 = caveolin 1; CLDN5 = claudin 5; SOX = SRY (sex-determining region on the Y chromosome)–related high-mobility group box; ZO-1 = zonula occludens 1.

previously shown that SOX18 enhances endothelial barrier function by upregulating the tight junction protein CLDN5 in pulmonary arterial endothelial cells (7). Thus, we next investigated whether the LPS-mediated downregulation of *Sox18* affected CLDN5 levels in the mouse lung and in HLMVECs. *Cldn5* mRNA expression (Figure 1E) and protein levels (Figure 1F) were significantly decreased in the lungs of mice treated with LPS compared with vehicle-treated mouse lungs. Similarly, in HLMVECs exposed to LPS (1 EU/ml) for 4 h, *CLDN5* mRNA (Figure 1G) and protein (Figure 1H) levels were also reduced. Immunofluorescence analysis was used to evaluate changes in the paracellular and transcellular pathways (Figure 1I). The data indicate that LPS decreased CLDN5 levels significantly (Figures 1J and 1K) but did not change total VE-cadherin (CDH5) levels (Figures 1L and 1M). However, the expression pattern of VE-cadherin was altered whereby cell border expression was predominantly lost (Figure 1L). Simultaneous phalloidin staining identified a significant increase in gap formation (Figures 1L and 1N). Furthermore, LPS significantly reduced ZO-1 staining, indicating a loss of tight junction formation (Figures 1O and 1P). Immunofluorescence staining for caveolin 1 identified a nonsignificant increase, suggesting that transcellular transport was unaffected by LPS under these conditions compared with the paracellular pathway (Figures 1I, 1O, and 1Q).

SOX18 Overexpression Prevents LPS-mediated Decrease in CLDN5 Protein Levels in HLMVECs

To evaluate the role of LPS-mediated SOX18 downregulation in endothelial cell permeability, we overexpressed the SOX18 transcription factor in HLMVECs exposed to LPS (Figure 2A) and found that SOX18 overexpression attenuated the LPS-induced decrease in endothelial barrier function (Figure 2B). Furthermore, overexpression of SOX18 in HLMVECs enhanced CLDN5 protein levels in the presence and absence of LPS (Figure 2C). To determine whether the protective effect of SOX18 overexpression on the endothelial barrier in the presence of LPS is mediated by CLDN5, SOX18 was overexpressed in HLMVECs before LPS exposure while CLDN5 expression was simultaneously silenced using a specific siRNA (Figure 2D). CLDN5 depletion in HLMVECs abolished the barrier-protective effect of SOX18 overexpression in the presence of LPS (Figure 2E). These findings suggest that LPS decreases SOX18 and CLDN5 levels, which in turn disrupts the endothelial barrier. In addition, the overexpression of SOX18 in an unrelated cell line (COS-7) is sufficient to increase CLDN5 promoter activity (*see* Figure E1 in the data supplement).

Gene Delivery of SOX18 to the Mouse Lung Attenuates Lung Permeability in ALI

To determine whether restoring SOX18 expression and enhancing CLDN5 levels can ameliorate the vascular hyperpermeability and lung damage in ALI, we used a polyethylenimine derivative transfection reagent to deliver pCMV6-SOX18 plasmid into the mouse lung via tail vein injection. Two days after gene delivery, mice received either saline (vehicle) or LPS (2 mg/kg) for 24 hours. Initial experiments confirmed a significant increase in SOX18 (Figure 3A) and CLDN5 (Figure 3B) protein levels in mouse lung in the presence and absence of LPS. Interestingly, overall SOX18 expression in the mouse lung in which SOX18 was overexpressed still declined after LPS exposure (Figure 3A), probably owing to the decrease in expression of endogenous SOX18. BAL fluid analysis indicated that SOX18 overexpression significantly attenuated LPS-induced cellular infiltration (Figure 3C) and protein extravasation (Figure 3D) into the lung airspaces. Using myeloperoxidase activity, we found that LPS-induced neutrophil infiltration was reduced in the lungs of SOX18-overexpressing mice (Figure 3E). In addition, we found that SOX18 overexpression significantly attenuated LPS-induced vascular leak, as indicated by a reduction in the extravasation of Evans Blue dye (Figure 3F). SOX18 overexpression did not appear to directly alter the expression of inflammation-related genes as determined using transcriptome-wide scanning of gene expression patterns on an Affymetrix microarray platform (Figure E2).

Gene Delivery of SOX18 to the Mouse Lung Prevents Lung Injury and Preserves Lung Mechanics in ALI

Lung sections stained with myeloperoxidase and hematoxylin and eosin indicated that increased SOX18 expression protected mouse lungs against LPS-induced histopathological changes characterized by edematous thickening of the alveolar septa, hyaline membrane formation, the infiltration of leukocytes, the presence of red blood cells in the alveolar and interstitial spaces, and debris accumulation in the alveoli (Figure 4A). A semiquantitative histopathological scoring system (13) was also used to assess the severity of the lung injury by evaluating the extent of intra-alveolar neutrophil permeation, alveolar septal thickening, fibrin accumulation filling the airspaces, and the presence of hyaline membranes. SOX18 overexpression attenuated the Lung Injury Score in the LPS-treated mice (Figure 4B). An analysis of lung mechanics revealed that SOX18 overexpression prevented the LPS-induced downward displacement of the pressure–volume curve (Figure 4C). Finally, we found that SOX18 overexpression significantly improved lung mechanics, as indicated by increased lung compliance (Figure 4D), decreased lung elastance (Figure 4E), decreased lung resistance (Figure 4F), and higher oxygen saturation (Figure 4G).

NF-κB (p65) Is Recruited to the SOX18 Promoter and Decreases SOX18 Promoter Activity during LPS Exposure

To determine the mechanism by which LPS downregulates SOX18 expression, the SOX18 promoter (−1,600 bp) was cloned into a pGL3 luciferase reporter vector (Figure 5A). Analysis of the *SOX18* promoter sequence using MatInspector revealed two NF-κB (p50/p65) binding sites and one NF-κB (c-Rel/p65) binding site (defined as sites 1–3) (14). After 48 hours of transfection with the SOX18 promoter construct, the HLMVECs were exposed to LPS (1 EU/ml) for 4 hours in the presence or absence of an NF-κB (p65) inhibitor, JSH-23 (4-methyl-N^1-[3-phenylpropyl] benzene-1,2-diamine; 16 μM). LPS exposure decreased SOX18 promoter activity; however, the inhibition of NF-κB attenuated the LPS-mediated decrease in SOX18 promoter activity (Figure 5B). Chromatin immunoprecipitation (ChIP) analysis demonstrated that LPS promoted the binding of NF-κB (p65) to the endogenous *SOX18* promoter at site 1 (−1,082 to −1,073 bp upstream of +1) in HLMVECs (Figure 5C). Furthermore, the mutation of NF-κB binding site 1 from

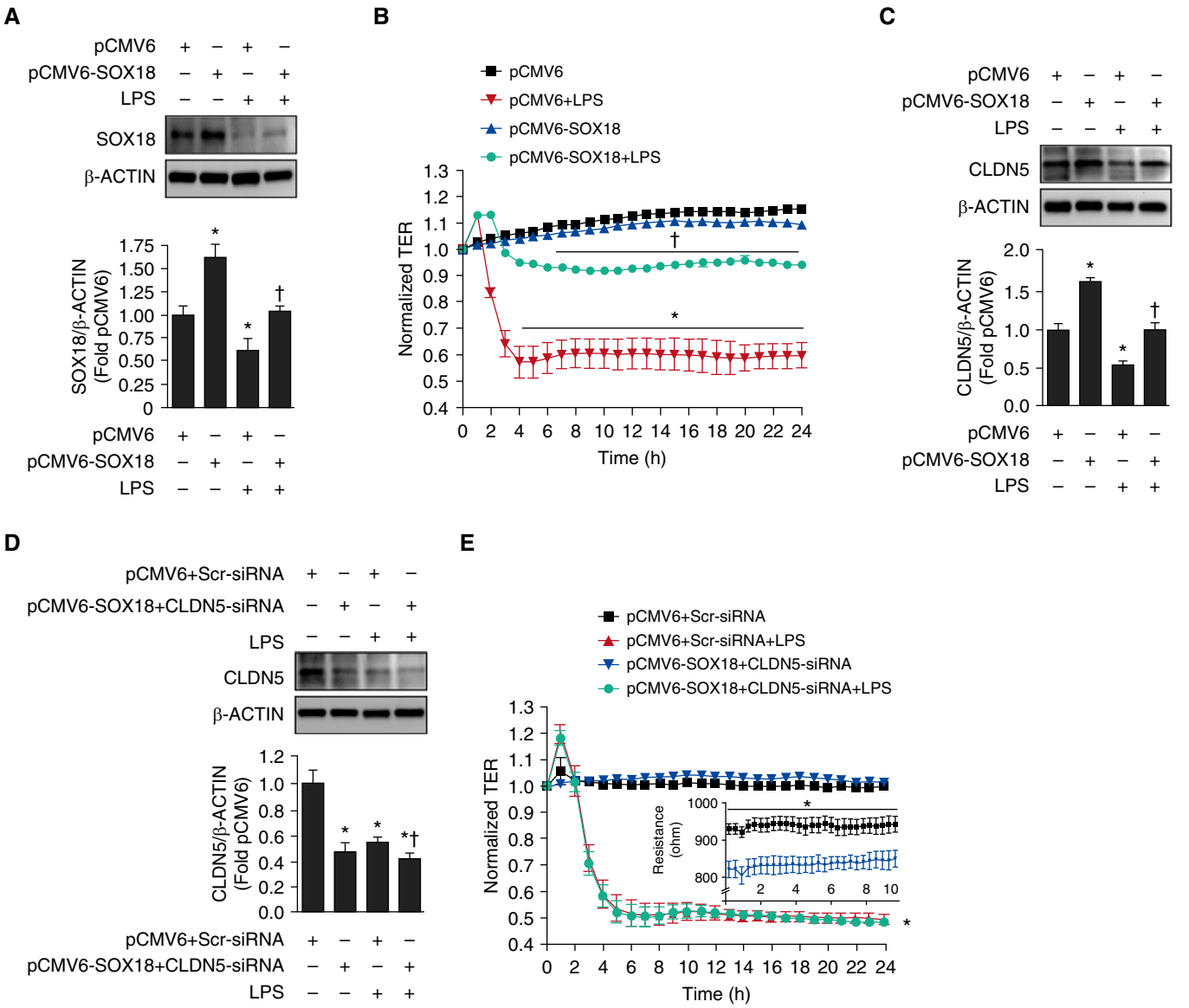

Figure 2. SOX18-mediated increases in CLDN5 protein levels protect against LPS-induced barrier dysfunction in HLMVECs. HLMVECs were transfected with either pCMV6 or pCMV6-SOX18 for 48 hours and then exposed to LPS (1 EU/ml) for 4 hours. (*A* and *C*) Immunoblot analysis indicated that SOX18 and CLDN5 protein levels were increased in HLMVECs transfected with pCMV6-SOX18 for 48 hours in the presence or absence of LPS (1 EU/ml; 4 h). HLMVEC monolayers grown on gold microelectrodes were transfected with either pCMV6 or pCMV6-SOX18 or pCMV6-SOX18 and a CLDN5 siRNA. After 48 hours, the cells were challenged with LPS (1 EU/ml; 0–24 h). (*B*) The normalized transendothelial resistance (TER) gradually decreased in response to LPS in pCMV6-transfected cells, whereas in the cells overexpressing SOX18, the decrease in TER was significantly attenuated. (*D*) The silencing of CLDN5 expression attenuated the protective effect of SOX18 overexpression. (*E*) However, the barrier-protective effect of SOX18 overexpression completely disappeared. Values are mean ± SEM; $n = 4$–6. $^{*}P < 0.05$ versus pCMV6 or pCMV6 + scrambled siRNA; $^{\dagger}P < 0.05$ versus pCMV6 + LPS.

GGGAGCCTCC to CTCAGCCTTT abolished the LPS-dependent decrease in SOX18 promoter activity (Figure 5D).

NF-κB Activity Is Stimulated by Peroxynitrite during LPS Exposure

We have recently shown that reducing peroxynitrite generation can attenuate inflammatory signaling during LPS exposure (15). Thus, we evaluated the role of peroxynitrite in stimulating NF-κB activity. We have previously shown that the nuclear factor of κ light polypeptide gene enhancer in B cells inhibitor-α (IκBα) protein is susceptible to nitration at tyrosine (Y)^{181} and Y^{305} and that this reduces the ability of IκBα to negatively regulate NF-κB activity (16). Our mass spectrometric data indicated that LPS induces the oxidation and nitration of Y^{305}; however, Y^{181} nitration was not detected (Figure 6A). To further evaluate the role of nitration in NF-κB activation, we evaluated phosphorylated p65 levels in LPS-challenged endothelial cells in the presence or absence of the peroxynitrite scavenger MnTMPyP. Our

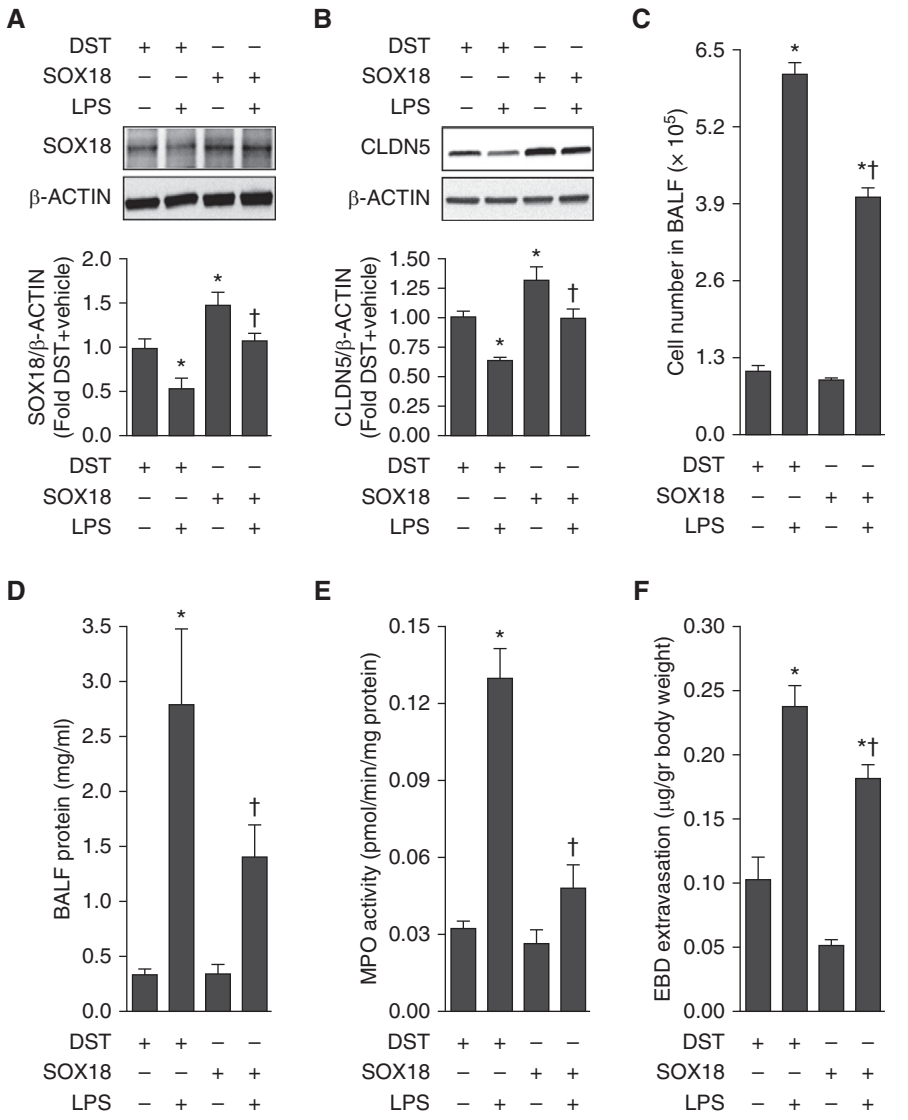

Figure 3. The overexpression of SOX18 in the mouse lung prevents LPS-induced pulmonary edema. Mice were injected with either DST-luciferase (DST) or pCMV6-SOX18 (SOX18) plasmid via the tail vein. After 48 hours, the mice received either saline (vehicle) or LPS (2 mg/kg body weight; 24 h) intratracheally. Protein extracts prepared from lung tissue homogenates were subjected to immunoblot analysis using specific antiserum raised against SOX18 and CLDN5. Densitometric analysis demonstrated a significant increase in (*A*) SOX18 and (*B*) CLDN5 protein levels in the presence and absence of LPS. (*C*) The total cell count in the BAL fluid (BALF) was elevated after LPS exposure, although this response was significantly decreased in the BALF of mice overexpressing SOX18. (*D*) SOX18 overexpression attenuated the LPS-mediated increase in BALF protein concentration and (*E*) lung myeloperoxidase (MPO) activity, which indicates neutrophil sequestration in the lung. (*F*) The capillary leak, as indicated by Evans Blue dye (EBD) extravasation in the lung and expressed as the ratio of EBD to body weight, induced by LPS was also significantly reduced in SOX18-overexpressing mice. Values are mean ± SEM; $n = 4$–6. *$P < 0.05$ versus DST + vehicle; †$P < 0.05$ versus DST + LPS.

data indicate that LPS stimulates the phosphorylation of p65 and that this is significantly reduced when peroxynitrite levels are decreased (Figure 6B). Similarly, peroxynitrite scavenging significantly attenuates the LPS-mediated activation of an NF-κB luciferase reporter promoter (Figure 6C), whereas exposing HLMVECs to a peroxynitrite donor alone is sufficient to increase the activity of the NF-κB luciferase reporter plasmid (Figure 6D).

Discussion

Our data show that *SOX18* mRNA expression and protein levels are reduced in the mouse lung exposed to LPS, supporting the conclusion that LPS downregulates *SOX18* expression via decreased transcription. In addition, we show in HLMVECs that *SOX18* expression is reduced by LPS in an NF-κB (p65)–dependent manner. A previous study showed that *SOX18* mRNA expression is reduced in human umbilical vein endothelial cells by the proinflammatory mediators TNF-α, IL-1, and LPS (12). The TNF-α–induced decrease in *SOX18* mRNA expression was similarly mediated by the p65 subunit of NF-κB (12). Using several *SOX18* promoter constructs of various lengths, it has been shown that the promoter region of *SOX18* susceptible to TNF-α–mediated repression is located within −0.2 kb to −1.0 kb from the transcriptional start site (12). We also found that the *SOX18* promoter region responsible for LPS-induced, NF-κB (p65)–dependent repression is located within −1.6 kb of the transcriptional start site. Interestingly, whereas analysis of the *SOX18* promoter using MatInspector revealed the presence of several potential NF-κB binding sites, ChIP analysis indicated that LPS increased NF-κB (p65) binding to the SOX18 promoter only at site 1 (−1,082 to −1,073 bp upstream). Furthermore, the mutation of NF-κB (p65) binding site 1 prevented the LPS-mediated decrease in SOX18 promoter activity. ChIP analyses also identified a decrease in NF-κB binding to site 2. The significance of these data is unclear because mutating site 1 is sufficient to attenuate LPS-mediated decreases in SOX18 promoter activity. We speculate that there may be cooperativity between sites 1 and 2 in the regulation of SOX18 promoter activity. However, further studies are required to test this possibility.

NF-κB is an inducible transcription factor that binds to the decameric nucleotide sequence GGGACTTTCC (17) and regulates the expression of many genes involved in immune and inflammatory responses (18). There are five NF-κB family members: p65 (RelA), RelB, c-Rel, p50 (NF-κB1), and p52 (NF-κB2) (18). The NF-κB subunits can homo- or heterodimerize through the Rel homology domain (19). Although all NF-κB members are able to

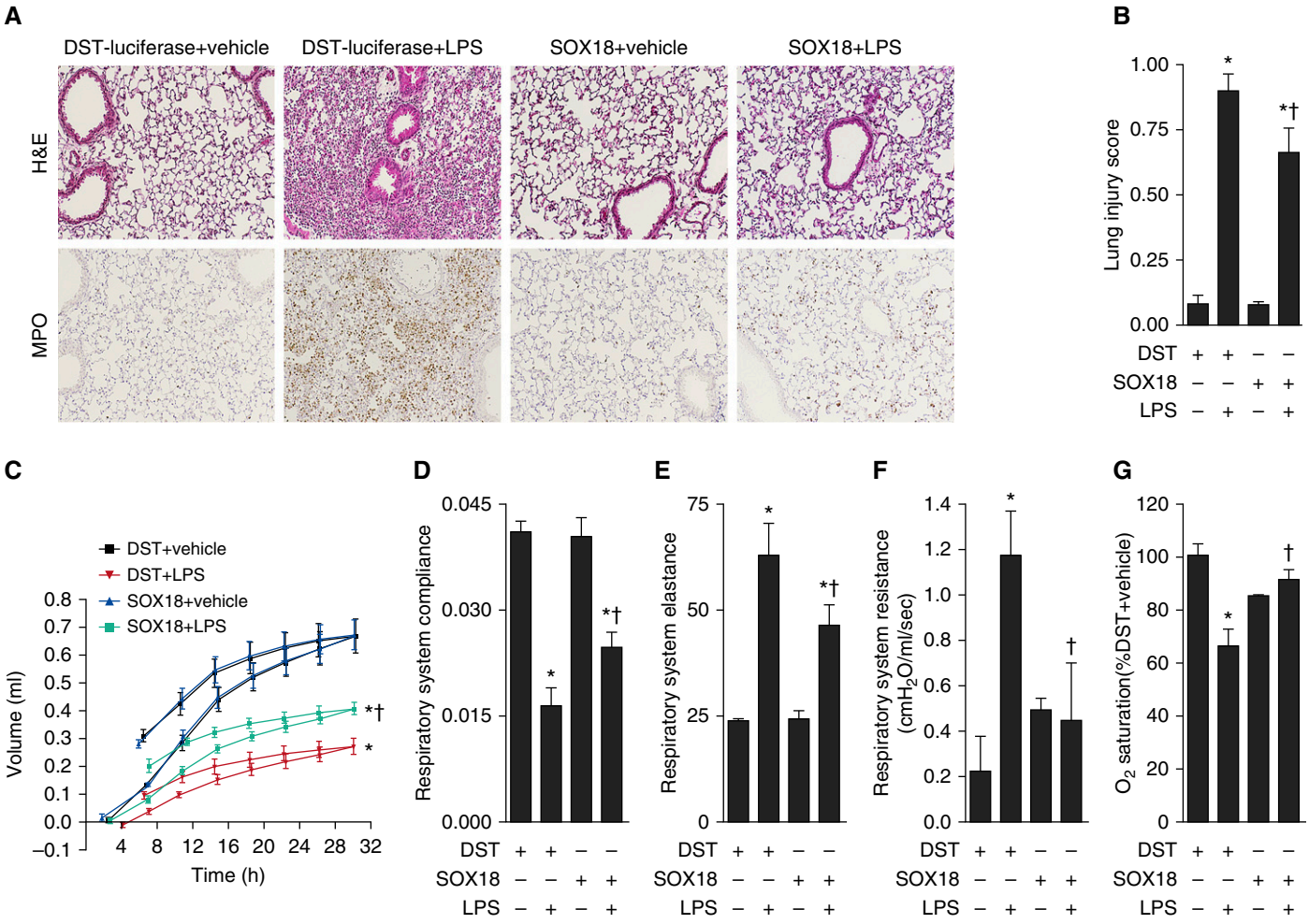

Figure 4. The overexpression of SOX18 in the mouse lung attenuates LPS-mediated lung injury and the disruption of lung mechanics. Mice were injected with either DST or SOX18 plasmid via the tail vein. After 48 hours, the mice received either saline (vehicle) or LPS (2 mg/kg body weight; 24 h) intratracheally. Lung sections were examined for signs of inflammation after hematoxylin and eosin staining (*A*), neutrophil infiltration after MPO staining (*A*) (representative micrographs are shown), and scored for lung injury (*B*). The inflammatory response induced by LPS is reduced in SOX18-overexpressing mice, as indicated by (*A*) significantly less lung MPO staining and (*B*) a lower Lung Injury Score. Additional mice were anesthetized 24 hours after LPS exposure, and the area around the throat was shaved. Transcutaneous oxygen saturation was monitored via a pulse oximeter placed on the neck. Subsequently, the mice were intubated, connected to a flexiVent ventilator (SCIREQ), and then lung mechanics were assessed. (*C*) The analysis of dynamic pressure–volume relationships in the mouse lung indicated that LPS caused a displacement of the pressure–volume curve to lower lung volumes, which was attenuated in SOX18-overexpressing mice. These data show that, for a given amount of pressure, LPS-exposed, SOX18-overexpressing mice experienced a higher V_T. The data represent pressure–volume loops for four groups with two curves: one for inhalation and one for exhalation events. SOX18-overexpressing mice given LPS also had (*D*) increased total respiratory compliance, (*E*) decreased total respiratory elastance, (*F*) decreased total respiratory resistance, and (*G*) higher oxygen saturation compared with LPS-exposed DST mice. Values are mean ± SEM; $n = 4$–6. $^*P < 0.05$ versus DST+vehicle; $^\dagger P < 0.05$ versus DST+LPS. H&E = hematoxylin and eosin; V_T = tidal volume.

bind DNA, only p65, RelB, and c-Rel have C-terminal transactivation domains (19). The activity of NF-κB is regulated primarily through interactions with inhibitory IκB proteins. The best-studied NF-κB–IκB interaction is that of IκBα with the NF-κB p50-RelA (p65) dimer (20). The presence of a nuclear export signal in IκBα results in the NF-κB complex being localized primarily to the cytoplasm, attenuating the ability of NF-κB to bind to DNA and regulate transcription. Thus, a key step in controlling the activity of NF-κB is regulating the IκB–NF-κB interaction. In the classical or canonical pathway, activation of an IκB kinase complex leads to the serine phosphorylation of IκBα, targeting it for degradation (21). The exposed NF-κB complex can then enter the nucleus and activate target gene expression. One of the target genes activated by NF-κB is IκBα (22). This newly synthesized IκBα enters the nucleus and removes NF-κB bound to DNA. The complex is then exported back to the cytoplasm, and the original latent state is restored. In this manner, the activation of the NF-κB pathway is a highly regulated, transient process, lasting approximately 30–60 minutes in most cells (23, 24).

Our data suggest that nitration also activates NF-κB in a noncanonical manner. This is in agreement with our earlier studies

A

5′ GTCTGTGAACGAGGTGCTAGGCCCGTGGGGCAAACTGGAGGGACGGGAGATCTGGAGACCAGACTGGGAGACCCAGCCCCGTATGCTGG
GACGATGGGCGTCGAGACAGACTGTGATGTGGGGCTTTGGGGAGGGCTGGACACCGACCGCGACAGCCCTCGGTGGGAGTGCCCCTGTGGG
GGTGCTGGCCTCAGGGCAGGAGTGCCCCTGGGGACAGTTCAGGAACAGCCTCTAAGGGGCACTGCAAGGCCCACGTGGGGCCCACCCCATT
CATAACACAGGCTGGATGTGGCCTAGCGAGGCTGGCAGGGACAGAGAACCAAGAGCTTCTGGCCACACAGGCTCAGGGTCACAAGACCTGT
GGCCTCTACCCATGGGGCTCCCGGCATAGTGTGGCGGGGGGAGCTG**GGGAGCCTCC**AGGCTATGAGGAGATGTGCCGCGAGGTGGCG
AGATTCTGACCCTGCCTGGAGGGCTGCTGGGGACACCCAACCCTTCTCCAGTAGAACCATGCGTGGCAGTGGGAGGGGAGGACCTCCAGAG
GGAGACCCTCAGCTCTGGAGCCCAGATCCCCTCCTGATGGAGTAGGAAGGGGACAGTGAAAATTCAGGAAGCTGGACGCTCCTCCGGAACC
CGCCCCCGCCCAGGTCAGAGGGTCCAGGGAGGGGCCAGTGGGAAGGACCCAGGTAGGCCCTGCCTCTTGCTGCAGCGGTGGCCTGGGCTGG
GCAGGGGAGCCAGCAAGCCACTGAGGGTCCCAGCCCCTTCCCCAAGGGCCCTTGGGGGGCAGGGAGGACGCCACAGCCTCTGCGTCCCTGC
TCCCCCTTCTCTTTGTGGGCTCCGTCCAGGGCCTCTGCTCTCTCCCTCCCTGTGTCAGCTTTGCCTTGTGCCAGAGTTGGTTTGGGAGTGA
GGACAGAAGACCATCTTGTCCCATAAAGGCACTCAAAGTCCCTGGTGCTGACGGTTACACATGGGTGTAGAGTTTCCAGCATGGGCGCCCC
TGGGGACTCAGAGCGCCTCCCCAAAGACGGGGCCTTTTCTGAAGGCGCTGCACTCCAGGAAGGACTTACCGGCTGTTGGGAAGGCAGCCTC
CCCAGAACTTGGTGTGAAAAAGGGCCCTCTCCTCCCCA**TGGAGCCTCC**CAGCGGGGGGCGGGGAACGGCAACCAGCGGGACACTGCC
GCCCTCCCCCAGTTACTGCCCGGGGGTCCGACTCCGTGGGTGGGTGGCAGCTCGCCTCCGAAAGTCTGGCAGCACCGGCCCTCATCAGCAG
CCCTTTCTTTCCCACCCGGGGGGTCTCTCCTTCTGAGAGGTCGCGGGGGAGGTGGGGGGGCTGTGCGCGGGGGAGGCCTCAGCGGAATCCC
GCCCGGCCTGAGAAGAAA**GGGAGCCCCC**GGGGAGGAGGCGGCCCCGACCCGCCCCCGCCCGCCCGCCCCGCCGCCGATTGGCCCTGA
GCCGCTATATCTGGGCGCCCGCCCGGCCCGAGGCCACCGCCGTCCCCACCGCCATCCGCCCTCCCGGCCTGGCCTGCCCTTGCGCCCGGCT
CCCCAGTGCCCGCCGCCCGCCCGCCGCGCTCCCGCGCTCCGTTCCGCCCAGGCCGCGCCCAGCTGGA ATG-3′

B

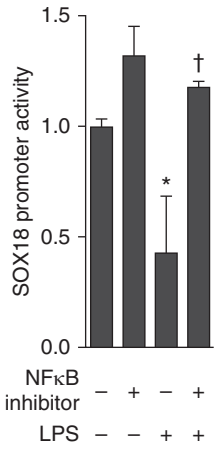

C

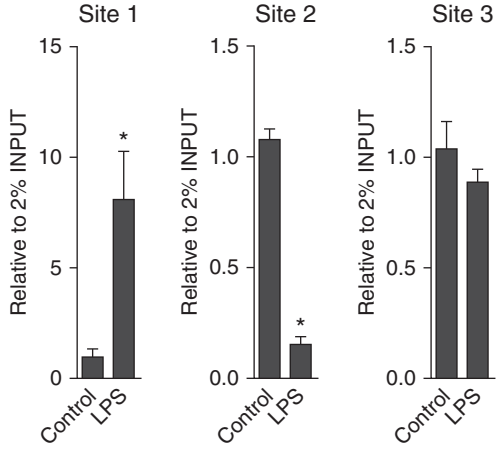

D

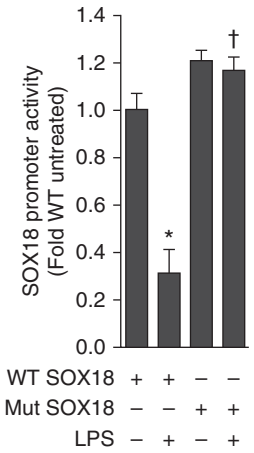

Figure 5. NF-κB (p65) binding decreases SOX18 promoter activity during LPS exposure in HLMVECs. The *SOX18* promoter sequence (−1,600 base pairs [bp]) with the potential NF-κB binding sites highlighted in bold. (*A*) HLMVECs were cotransfected with the SOX18 luciferase promoter plasmid and β-galactosidase plasmid. After 36 hours, the HLMVECs were treated with the NF-κB inhibitor JSH-23 (1 endotoxin unit/ml; 4 h). The luciferase activity and β-galactosidase activity in cell lysates was measured, and the ratio of luciferase activity to β-galactosidase activity was used to determine the SOX18 promoter activity. (*B*) SOX18 promoter activity was decreased in LPS-treated HLMVECs, which was prevented by the inhibition of NF-κB. (*C*) Chromatin immunoprecipitation analysis in LPS-treated HLMVECs indicated increased p65 NF-κB binding to site 1 (−1,082 to −1,073 bp) within the SOX18 promoter. The NF-κB (p65) binding site 1 in the wild-type (WT) SOX18 promoter construct was mutated from GGGAGCCTCC to CTCAGCCTTT to generate a mutant SOX18 promoter construct. HLMVECs were cotransfected with either the wild-type SOX18 promoter or the mutant SOX18 promoter along with β-galactosidase plasmid for 48 hours and exposed to LPS (1 endotoxin unit/ml; 4 h). (*D*) SOX18 promoter activity was preserved in HLMVECs transfected with the mutant NF-κB binding site 1 promoter construct in the presence of LPS. Values are mean ± SEM; $n = 4$–7. *$P < 0.05$ versus untreated; †$P < 0.05$ versus LPS.

that demonstrated blocking protein nitration reduces inflammatory signaling mediated through NF-κB (10, 15, 25, 26). The present study further demonstrates that NF-κB activation during LPS exposure is significantly attenuated (up to a 40% reduction) when peroxynitrite levels are reduced. Furthermore, our data suggest that the mechanism by which this occurs is via the nitration of IκBα at Y^{305}. These data are in partial agreement with a prior study in which ionizing radiation stimulated NF-κB activity via IκBα nitration at Y^{181} and Y^{305}, leading to the dissociation from NF-κB (16), although Y^{181} nitration was not observed in LPS-challenged HLMVECs. The sustained activation of NF-κB in the lung during ARDS produces a so-called cytokine storm and a severe inflammatory response. The reasons for this prolonged activation are unresolved. However, nitration is a covalent modification that adds a nitro group to one ortho carbon of tyrosine's phenolic ring to form 3-nitrotyrosine. As such, the 3-nitrotyrosine group cannot be removed until the protein is degraded, resulting in loss of normal

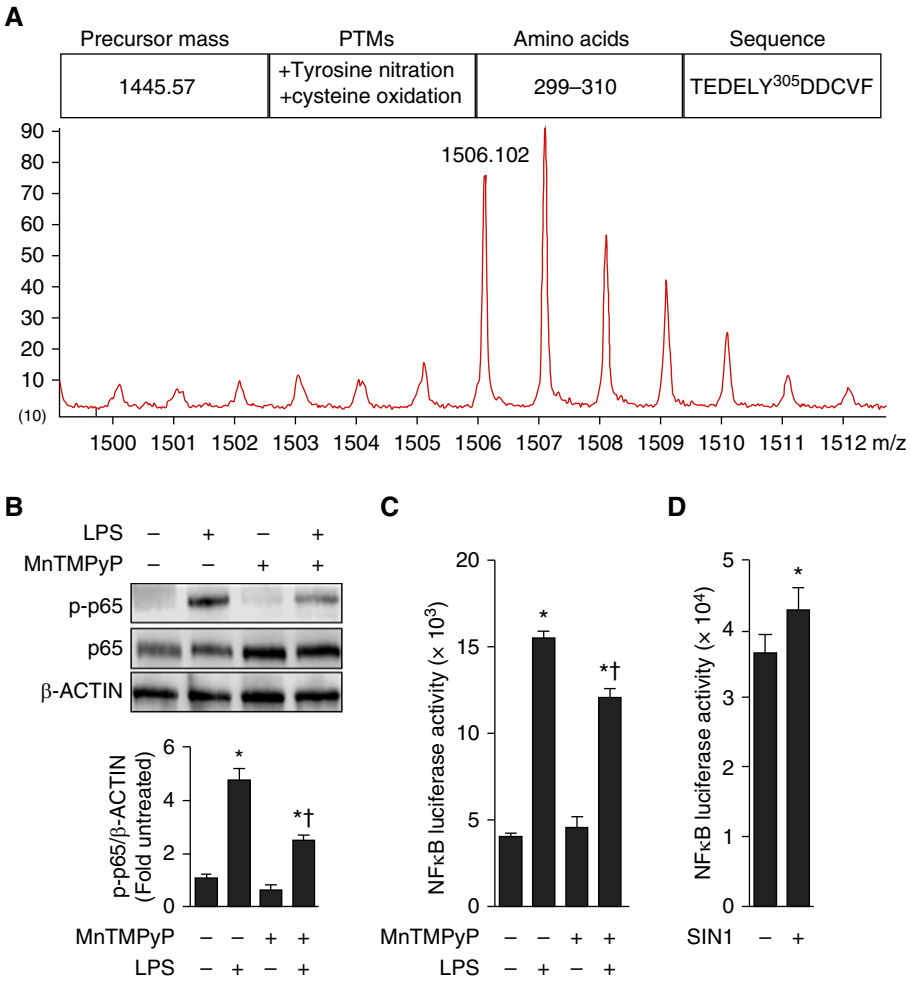

Figure 6. Peroxynitrite-mediated nitration is involved in the activation of NF-κB (p65) during LPS exposure in HLMVECs. HLMVECs were exposed to LPS (1 EU/ml) for 4 hours and IκBα (nuclear factor of κ light polypeptide gene enhancer in B cells inhibitor, α) protein was immunoprecipitated and subjected to mass spectrometric analysis. (*A*) A single tyrosine residue located at tyrosine (Y)^{305} was identified as being oxidized and nitrated. HLMVECs were also exposed to the peroxynitrite scavenger MnTMPyP (25 μM; 30 min pretreatment), then exposed to LPS (2 EU/ml) for 2 hours. (*B*) The level of NF-κB activation was then estimated by using immunoblot analysis to measure changes in phosphorylated p65 levels. LPS significantly increased phosphorylated p65 levels, and this was attenuated in the presence of MnTMPyP. HLMVECs were transiently transfected with a NF-κB luciferase reporter plasmid (48 h), then exposed to LPS (2 EU/ml; 8 h) or the peroxynitrite donor SIN-1 (1 mM) for 1 hour. (*C* and *D*) LPS significantly increased luciferase activity, and this was attenuated in the presence of MnTMPyP. Peroxynitrite alone is able to increase the activity of the NF-κB luciferase reporter plasmid. Values are mean ± SEM; $n = 3$ (*B–D*). $^{*}P < 0.05$ versus untreated; $^{\dagger}P < 0.05$ versus LPS alone. PTMs = post-translational modifications.

physiological regulation. This is similar to that observed for NF-κB signaling during ARDS. Thus, although speculative, this could explain, at least in part, the aberrant temporal activation of NF-κB during ARDS and could potentially be a therapeutic target for treating the disease.

Although NF-κB (p65) activation is typically associated with promoting transcription during ALI, recent reports suggest that NF-κB (p65) also functions as a transcriptional repressor under cytotoxic stimuli such as ultraviolet light (27), doxorubicin (27), and TNF-α (28–32). Although the mechanism by which NF-κB–mediated transcriptional repression is not fully understood, available evidence suggests that epigenetic regulation via class I HDACs 1, 2, and 3 (27) and DNA (cytosine-5)-methyltransferase-1 (DNMT-1) (32) can be involved. Indeed, it is becoming more apparent that epigenetic regulation plays a major role in regulating gene expression under both physiologic and pathologic conditions. Acetylation is an important post-translational modification of histones determining the accessibility of chromatin and hence gene transcription (33). It has been shown that NF-κB (p50, p65) interacts with HDAC1 through its p65/RelA domain (amino acids [aa] 1–276) to repress gene expression (34, 35). In addition, p50 interacts directly with HDAC1 (34). Interestingly, protein kinase A (PKA), a barrier-protective signal, phosphorylates NF-κB (p65), lowering its affinity with HDAC1 (34). HDAC2 is also recruited to NF-κB (p65) indirectly by binding to HDAC1 (35). However, whether NF-κB induces the transcriptional repression of *SOX18* via the recruitment of HDACs requires further study.

The regulation DNA methylation is another important epigenetic regulator of gene transcription. DNMT-1 is the most abundant DNA methyltransferase (36). The DNMT family members are classified as either *de novo* (DNMT-3A and DNMT-3B) or maintenance (DNMT-1) (37). As part of the DNA replication complex, DNMT-1 maintains the DNA methylation pattern of the newly synthesized DNA strand via the addition of a methyl group to the 5 position of the cytosine ring within the CpG dinucleotides (C5-methylcytosine) (36). DNA methylation is an important epigenetic modification that can become altered during disease states and lead to gene expression changes (37). CpG islands are frequently located in the vicinity of transcriptional start sites, and the methylation of DNA may physically impede the binding of transcriptional factors to the gene (38). In addition, methyl-CpG–binding domain proteins bind to methylated DNA and then recruit additional proteins, such as HDACs and other chromatin-remodeling proteins, to condense the chromatin structure (39). The inflammatory cytokine TNF-α represses gene expression in cancerous lung cells by inducing an interaction between NF-κB (p65) and DNMT-1 (32). The RelA domain (aa 109–119) of NF-κB (p65) was found to interact directly with DNMT-1 (32). Interestingly, a protein transduction domain RelA/p65 (aa 109–120) peptide prevented this interaction, promoted hypermethylation and NF-κB (p65)–mediated gene repression, and inhibited basal and TNF-α–stimulated

invasion of lung cancer cells (32). Again, the possible role of DNMT-1 in the downregulation of SOX18 by LPS requires future studies.

Claudins are vital in the assembly of a tight junctional complex with CLDN5-knockout mice selectively permeable to small molecules (<800 kD), suggesting that the remaining claudins form slightly larger pores (40). CLDN5 is dynamically regulated by several transcription factors. The present investigators (7) and others (41) have shown that CLDN5 expression and endothelial barrier function are increased by the transcription factor SOX18. However, other transcription factors can also regulate CLDN5. For example, a complex of T-cell factor 4, β-catenin, and Forkhead box protein O1 causes the repression of CLDN5 gene expression (42), as does vascular endothelial growth factor (43) and TNF-α/NF-κB (44). The expression of CLDN5 is upregulated by Krüppel-like factor 4 (45) and ETS-related gene (46). Thus, it is possible that in ALI, other transcription factors besides SOX18 may be involved in the downregulation of CLDN5. However, further studies are required to evaluate this possibility. CLDN5 can also be regulated in a post-translational manner. In particular, changes in its phosphorylation status can drastically regulate the barrier properties at the tight junction complex. For example, the secondary messenger cAMP induces the phosphorylation of CLDN5 on threonine residues via the activation of PKA, enhancing its membrane distribution and increasing endothelial barrier function (47). The activation of PKC isoforms (PKC-α and -ζ) under inflammatory conditions increases CLDN5 serine phosphorylation and induces the disappearance of CLDN5 from the cell membrane, increasing endothelial permeability (48). In addition, the Rho-associated protein kinase–mediated phosphorylation of CLDN5 on Thr^{207} results in increased endothelial permeability (49). Because RhoA/Rho-associated protein kinase signaling is enhanced by LPS, this could synergize with the loss of SOX18 to attenuate the barrier-protective effects of CLDN5.

In conclusion, our studies have identified a novel mechanism by which LPS attenuates pulmonary endothelial barrier function via the downregulation of the SOX18–CLDN5 axis. The fact that the gene delivery of SOX18 to the mouse lung attenuated the development of ALI in response to LPS challenge confirms the importance of this pathway in regulating the pulmonary endothelial barrier. Furthermore, these data, in conjunction with data derived from our earlier studies (7), implicate the SOX18–CLDN5 axis as a primary control point for endothelial paracellular permeability. This in turn influences inflammatory cell infiltration and transmigration, and when this axis is decreased, there is increased inflammatory lung injury and edema. Thus, we speculate that strategies aimed at augmenting the SOX18–CLDN5 pathway may be a new therapeutic approach to the treatment of ALI/ARDS. ■

Author disclosures are available with the text of this article at www.atsjournals.org.

References

1. Bernard GR, Artigas A, Brigham KL, Carlet J, Falke K, Hudson L, *et al*. The American-European Consensus Conference on ARDS: Definitions, mechanisms, relevant outcomes, and clinical trial coordination. *Am J Respir Crit Care Med* 1994;149:818–824.
2. Rubenfeld GD, Caldwell E, Peabody E, Weaver J, Martin DP, Neff M, *et al*. Incidence and outcomes of acute lung injury. *N Engl J Med* 2005; 353:1685–1693.
3. Ware LB, Matthay MA. The acute respiratory distress syndrome. *N Engl J Med* 2000;342:1334–1349.
4. Hudson LD, Milberg JA, Anardi D, Maunder RJ. Clinical risks for development of the acute respiratory distress syndrome. *Am J Respir Crit Care Med* 1995;151:293–301.
5. Lien E, Means TK, Heine H, Yoshimura A, Kusumoto S, Fukase K, *et al*. Toll-like receptor 4 imparts ligand-specific recognition of bacterial lipopolysaccharide. *J Clin Invest* 2000;105:497–504.
6. Pittet JF, Mackersie RC, Martin TR, Matthay MA. Biological markers of acute lung injury: prognostic and pathogenetic significance. *Am J Respir Crit Care Med* 1997;155:1187–1205.
7. Gross CM, Aggarwal S, Kumar S, Tian J, Kasa A, Bogatcheva N, *et al*. Sox18 preserves the pulmonary endothelial barrier under conditions of increased shear stress. *J Cell Physiol* 2014;229:1802–1816.
8. Irrthum A, Devriendt K, Chitayat D, Matthijs G, Glade C, Steijlen PM, *et al*. Mutations in the transcription factor gene *SOX18* underlie recessive and dominant forms of hypotrichosis-lymphedema-telangiectasia. *Am J Hum Genet* 2003;72:1470–1478.
9. Pennisi D, Gardner J, Chambers D, Hosking B, Peters J, Muscat G, *et al*. Mutations in *Sox18* underlie cardiovascular and hair follicle defects in ragged mice. *Nat Genet* 2000;24:434–437.
10. Aggarwal S, Gross CM, Kumar S, Dimitropoulou C, Sharma S, Gorshkov BA, *et al*. Dimethylarginine dimethylaminohydrolase II overexpression attenuates LPS-mediated lung leak in acute lung injury. *Am J Respir Cell Mol Biol* 2014;50:614–625.
11. Catravas JD, Snead C, Dimitropoulou C, Chang AS, Lucas R, Verin AD, *et al*. Harvesting, identification and barrier function of human lung microvascular endothelial cells. *Vascul Pharmacol* 2010;52:175–181.
12. Basílio J, Hoeth M, Holper-Schichl YM, Resch U, Mayer H, Hofer-Warbinek R, *et al*. TNFα-induced down-regulation of Sox18 in endothelial cells is dependent on NF-κB. *Biochem Biophys Res Commun* 2013;442:221–226.
13. Matute-Bello G, Winn RK, Jonas M, Chi EY, Martin TR, Liles WC. Fas (CD95) induces alveolar epithelial cell apoptosis in vivo: implications for acute pulmonary inflammation. *Am J Pathol* 2001; 158:153–161.
14. Cartharius K, Frech K, Grote K, Klocke B, Haltmeier M, Klingenhoff A, *et al*. MatInspector and beyond: promoter analysis based on transcription factor binding sites. *Bioinformatics* 2005;21:2933–2942.
15. Gross CM, Rafikov R, Kumar S, Aggarwal S, Ham PB III, Meadows ML, *et al*. Endothelial nitric oxide synthase deficient mice are protected from lipopolysaccharide induced acute lung injury. *PLoS One* 2015; 10:e0119918.
16. Yakovlev VA, Barani IJ, Rabender CS, Black SM, Leach JK, Graves PR, *et al*. Tyrosine nitration of IκBα: a novel mechanism for NF-κB activation. *Biochemistry* 2007;46:11671–11683.
17. Sen R, Baltimore D. Multiple nuclear factors interact with the immunoglobulin enhancer sequences. *Cell* 1986;46:705–716.
18. Ghosh S, May MJ, Kopp EB. NF-κB and Rel proteins: evolutionarily conserved mediators of immune responses. *Annu Rev Immunol* 1998;16:225–260.
19. Verma IM, Stevenson JK, Schwarz EM, Van Antwerp D, Miyamoto S. Rel/NF-κB/IκB family: intimate tales of association and dissociation. *Genes Dev* 1995;9:2723–2735.
20. Ghosh S, Karin M. Missing pieces in the NF-κB puzzle. *Cell* 2002;109 (Suppl):S81–S96.
21. Hinz M, Scheidereit C. The IκB kinase complex in NF-κB regulation and beyond. *EMBO Rep* 2014;15:46–61.
22. Chen F, Castranova V, Shi X. New insights into the role of nuclear factor-κB in cell growth regulation. *Am J Pathol* 2001;159: 387–397.

23. Baeuerle PA. IκB-NF-κB structures: at the interface of inflammation control. *Cell* 1998;95:729–731.
24. Baeuerle PA. Pro-inflammatory signaling: last pieces in the NF-κB puzzle? *Curr Biol* 1998;8:R19–R22.
25. Sharma S, Smith A, Kumar S, Aggarwal S, Rehmani I, Snead C, *et al*. Mechanisms of nitric oxide synthase uncoupling in endotoxin-induced acute lung injury: role of asymmetric dimethylarginine. *Vascul Pharmacol* 2010;52:182–190.
26. Rafikov R, Dimitropoulou C, Aggarwal S, Kangath A, Gross C, Pardo D, *et al*. Lipopolysaccharide-induced lung injury involves the nitration-mediated activation of RhoA. *J Biol Chem* 2014;289:4710–4722.
27. Campbell KJ, Rocha S, Perkins ND. Active repression of antiapoptotic gene expression by RelA(p65) NF-κB. *Mol Cell* 2004;13:853–865.
28. Kouba DJ, Chung KY, Nishiyama T, Vindevoghel L, Kon A, Klement JF, *et al*. Nuclear factor-κB mediates TNF-α inhibitory effect on α2(I) collagen (COL1A2) gene transcription in human dermal fibroblasts. *J Immunol* 1999;162:4226–4234.
29. Shaw J, Zhang T, Rzeszutek M, Yurkova N, Baetz D, Davie JR, *et al*. Transcriptional silencing of the death gene BNIP3 by cooperative action of NF-κB and histone deacetylase 1 in ventricular myocytes. *Circ Res* 2006;99:1347–1354.
30. Kim S, Domon-Dell C, Kang J, Chung DH, Freund JN, Evers BM. Down-regulation of the tuor suppressor PTEN by the tumor necrosis factor-α/nuclear factor-κB (NF-κB)-inducing kinase/NF-κB pathway is linked to a default IκB-α autoregulatory loop. *J Biol Chem* 2004;279:4285–4291.
31. Xia D, Srinivas H, Ahn YH, Sethi G, Sheng X, Yung WK, *et al*. Mitogen-activated protein kinase kinase-4 promotes cell survival by decreasing PTEN expression through an NFκB-dependent pathway. *J Biol Chem* 2007;282:3507–3519.
32. Liu Y, Mayo MW, Nagji AS, Smith PW, Ramsey CS, Li D, *et al*. Phosphorylation of RelA/p65 promotes DNMT-1 recruitment to chromatin and represses transcription of the tumor metastasis suppressor gene *BRMS1*. *Oncogene* 2012;31:1143–1154.
33. Knoepfler PS, Eisenman RN. Sin meets NuRD and other tails of repression. *Cell* 1999;99:447–450.
34. Zhong H, May MJ, Jimi E, Ghosh S. The phosphorylation status of nuclear NF-κB determines its association with CBP/p300 or HDAC-1. *Mol Cell* 2002;9:625–636.
35. Ashburner BP, Westerheide SD, Baldwin AS Jr. The p65 (RelA) subunit of NF-κB interacts with the histone deacetylase (HDAC) corepressors HDAC1 and HDAC2 to negatively regulate gene expression. *Mol Cell Biol* 2001;21:7065–7077.
36. Luczak MW, Jagodziński PP. The role of DNA methylation in cancer development. *Folia Histochem Cytobiol* 2006;44:143–154.
37. Di Ruscio A, Ebralidze AK, Benoukraf T, Amabile G, Goff LA, Terragni J, *et al*. DNMT1-interacting RNAs block gene-specific DNA methylation. *Nature* 2013;503:371–376.
38. Choy MK, Movassagh M, Goh HG, Bennett MR, Down TA, Foo RS. Genome-wide conserved consensus transcription factor binding motifs are hyper-methylated. *BMC Genomics* 2010;11:519.
39. Nan X, Ng HH, Johnson CA, Laherty CD, Turner BM, Eisenman RN, *et al*. Transcriptional repression by the methyl-CpG-binding protein MeCP2 involves a histone deacetylase complex. *Nature* 1998;393:386–389.
40. Nitta T, Hata M, Gotoh S, Seo Y, Sasaki H, Hashimoto N, *et al*. Size-selective loosening of the blood-brain barrier in claudin-5-deficient mice. *J Cell Biol* 2003;161:653–660.
41. Fontijn RD, Volger OL, Fledderus JO, Reijerkerk A, de Vries HE, Horrevoets AJ. SOX-18 controls endothelial-specific claudin-5 gene expression and barrier function. *Am J Physiol Heart Circ Physiol* 2008;294:H891–H900.
42. Taddei A, Giampietro C, Conti A, Orsenigo F, Breviario F, Pirazzoli V, *et al*. Endothelial adherens junctions control tight junctions by VE-cadherin-mediated upregulation of claudin-5. *Nat Cell Biol* 2008;10:923–934.
43. Argaw AT, Gurfein BT, Zhang Y, Zameer A, John GR. VEGF-mediated disruption of endothelial CLN-5 promotes blood-brain barrier breakdown. *Proc Natl Acad Sci USA* 2009;106:1977–1982.
44. Aslam M, Ahmad N, Srivastava R, Hemmer B. TNF-α induced NFκB signaling and p65 (RelA) overexpression repress Cldn5 promoter in mouse brain endothelial cells. *Cytokine* 2012;57:269–275.
45. Ma J, Wang P, Liu Y, Zhao L, Li Z, Xue Y. Krüppel-like factor 4 regulates blood-tumor barrier permeability via ZO-1, occludin and claudin-5. *J Cell Physiol* 2014;229:916–926.
46. Yuan L, Le Bras A, Sacharidou A, Itagaki K, Zhan Y, Kondo M, *et al*. ETS-related gene (ERG) controls endothelial cell permeability via transcriptional regulation of the claudin 5 (CLDN5) gene. *J Biol Chem* 2012;287:6582–6591.
47. Ishizaki T, Chiba H, Kojima T, Fujibe M, Soma T, Miyajima H, *et al*. Cyclic AMP induces phosphorylation of claudin-5 immunoprecipitates and expression of claudin-5 gene in blood-brain-barrier endothelial cells via protein kinase A-dependent and -independent pathways. *Exp Cell Res* 2003;290:275–288.
48. Stamatovic SM, Dimitrijevic OB, Keep RF, Andjelkovic AV. Protein kinase Cα-RhoA cross-talk in CCL2-induced alterations in brain endothelial permeability. *J Biol Chem* 2006;281:8379–8388.
49. Yamamoto M, Ramirez SH, Sato S, Kiyota T, Cerny RL, Kaibuchi K, *et al*. Phosphorylation of claudin-5 and occludin by rho kinase in brain endothelial cells. *Am J Pathol* 2008;172:521–533.